May 11, 1999

Novel One-Phase Synthesis of Thiol-Functionalized Gold, Palladium, and Iridium Nanoparticles Using Superhydride

Chanel K. Yee, *New York University*
Rainer Jordan, *New York University*
Abraham Ulman, *New York University*
Henry White, *New York University*
Alexander H. King, *State University of New York at Stony Brook*, et al.

Novel One-Phase Synthesis of Thiol-Functionalized Gold, Palladium, and Iridium Nanoparticles Using Superhydride

Chanel K. Yee,[†,‡] Rainer Jordan,[†,‡] Abraham Ulman,*[,‡,||] Henry White,[†,§] Alexander King,[§] Miriam Rafailovich,[§] and Jonathan Sokolov[†,§]

Department of Chemical Engineering, Chemistry and Materials Science, Polytechnic University, Six Metrotech Center, Brooklyn, New York 11201, Department of Materials Sciences and Engineering, State University of New York at Stony Brook, Stony Brook, New York 11794-2275

Received January 7, 1999. In Final Form: February 25, 1999

A new, facile, general one-phase synthesis for thiol-functionalized gold, palladium, and iridium nanoparticles, using tetrahydrofuran (THF) as the solvent and lithium triethylborohydride (Superhydride) as the reducing agent, is presented. For octadecanethiol-functionalized gold (Au/ODT) nanoparticles, HRTEM of drop-cast particle-films revealed the formation of spherical particles of $d = 4 \pm 0.3$ nm average size. Electron diffraction shows fcc packing arrangement, similar to that of bulk gold. The crystalline gold cores are surrounded with closely packed *n*-alkyl chains mainly in an all-trans conformation, adopting orthorhombic packing as confirmed by FTIR spectroscopy. Particles are arranged in a discrete solidlike assembly with a correlation length of ~5 nm, as the interparticle distance (center-to-center) and a constant edge-to-edge distance of 1 nm as shown by FFT analysis. Using the same synthetic procedure gold nanoparticles functionalized with 11-hydroxyundecane-1-thiol and with 4′-bromo-4-mercaptobiphenyl were prepared. TEM images of drop-cast Pd/ODT and Ir/ODT nanoparticles show an average size of 2.25 nm for the former, while for the latter the distribution is broader with the majority of particles between 2.25 and 4.25 nm. Both nanoparticles are crystalline with fcc packing. FTIR spectroscopy reveals that octadecyl chains are close-packed in all-trans conformation, and that there is presumably one chain in unit cell.

Introduction

Submicrometer size materials have attracted a remarkable academic and industrial effort of research due to their potential applications ranging from fundamental studies in quantum physics, fabricating of composite materials, information storage/optoelectronics, and immunoassays to catalysts. A precise control of size and chemical behavior (stability *and* reactivity) by means of the synthesis itself is one of the main targets due to the direct correlation of intriguing new properties with the particle size, bridging the gap between molecules and bulk materials.[1]

In the past few years, there has been significant research in the area of nanoparticles. Semiconductors,[2] including silicon[3] and germanium,[3b] magnetic,[4] and different metallic nanoparticles such as iron,[5] cobalt,[5,6] nickel,[5,7] copper,[8] zinc,[9] rhodium,[10] ruthenium,[11] gold,[1b,f,12] and silver[12b,13] were prepared and studied.

A considerable effort was focused on systems of colloidal gold, for which a broad variety of synthetic procedures was reported.[1b,f] While native colloidal gold solutions are only stable for a restricted time, Brust et al.[14] were able to overcome this problem by developing a facile method for the in situ preparation of alkanethiol-stabilized gold

† NSF MRSEC for Polymers at Engineered Interfaces.
‡ Polytechnic University.
§ State University of New York at Stony Brook.
|| Telephone: 718-260-3119. Fax: 718-260-3125. E-mail: aulman@duke.poly.edu.

(1) The exponentially increasing number of publications demonstrates by itself the potential applications suitable for these new materials. For reviews on the different aspects refer to, e.g.: (a) Belloni, J. *Curr. Opin. Colloid Interface Sci.* **1996**, *2*, 184. (b) Brust, L. *Curr. Opin. Colloid Interface Sci.* **1996**, *2*, 197. (c) Matijevi'c, E. *Curr. Opin. Coll. Interface Sci.* **1996**, *1*, 176. (d) Haberland, H., Ed. *Clusters of atoms and molecules;* Springer-Verlag: New York, 1994. (e) *Clusters and Colloids. From Theory to Applications;* Schmid, G., Ed.; VCH: New York, 1994. (f) Schmidt, G. *Chem. Rev.* **1992**, *92*, 1709. (g) Lewis, L. N. *Chem. Rev.* **1993**, *93*, 2693. (h) *Optical Properties of Metal Clusters*; Kreibig, U.; Vollmer, M., Eds. Springer-Verlag: New York, 1995.

(2) (a) Kotov, N. A.; Dekany, I.; Fendler, J. H. *J. Phys. Chem.* **1995**, *99*, 13065. (b) Cusack, L.; Rizza, R.; Fitzmaurice, D. *Angew. Chem.* **1997**, *36*, 848. (c) Smirnova, N. P.; Kryukov, A. I.; Ogenko, V. M. *J. Mol. Struct.* **1997**, *408/409*, 563. (d) Khosravi, A. A.; Kundu, M.; Kulkarni, S. K. *Appl. Phys. Lett.* **1995**, *67*, 2506. (e) Mandal, B. M.; Banerjee, P. *Macromolecules* **1995**, *28*, 3940. (f) Ko, M.-J.; Birnboim, M.; Plawsky, J. *Adv. Mater.* SEP **1997**, *9*, 909. (g) Trindade, T.; O'Brien, P. *Adv. Mater.* **1996**, *8*, 161.

(3) (a) Seraphin, A. A.; Werwa, E.; Kolenbrander, K. D. *J. Mater. Res.* **1997**, *12*, 338. (b) Gorla, C. R.; Liang, S.; Lu, Y. *J. Vac. Sci. Technol.* **1997**, *15*, 860. (c) Tanenbaum, D. M.; Laracuente, A. L.; Gallagher, A. *Appl. Phys. Lett.* **1996**, *68*, 1705. (d) Cabarrocas, P. R.; Gay, P.; Hadjadj, A. *J. Vac. Sci. Technol.* **1996**, *14*, 655. (e) Powell, A. R.; LeGoues, F. K.; Iyer, S. S. *Jpn. J. Appl. Phys. Part 1* **1994**, *33*, 2392. (f) Koos, K.; Picsik, I.; Vazonyi, E. B. *Appl. Phys. Lett.* **1993**, *62*, 1797.

(4) (a) Tomanek, D.; Kim, S. G.; Hilf, E. R. *Z. Phys. D* **1997**, *40*, 539. (b) Ho, J. C.; Hamdeh, H. H.; Oliver, S. A. *Phys. Rev B: Condens. Matter.* **1995**, *52*, 10122. (c) Pillai, V.; Kumar, P.; Multani, M. S. *Colloids Surf.* **1993**, *80*, 69. (d) Ho, J. C.; Hamdeh, H. H.; Oliver, S. A. *Phys. Rev. B: Condens. Matter* **1995**, *52*, 10122. (e) Bakuzis, A. F.; Morais, P. C.; Tourinho, F. A. *J. Magn. Reson. Ser. A.* **1996**, *122*, 100. (f) Wernsdorfer, W.; Orozco, E.; B.; Barbara, B. *Phys. Rev. Lett.* **1997**, *79*, 4014.

(5) Seshadri, R.; Sen, R.; Rao, C. N. R. *Chem. Phys. Lett.* **1994**, *231*, 308.

(6) (a) Platonova, O. A.; Bronstein, L. M.; Antonietti, M. *Colloid Polym. Sci.: Kolloid-Zeitschrift* **1997**, *275*, 426. (b) Osuna, J.; de Caro, D.; Fert, A. *J. Phys. Chem.* **1996**, *100*, 14571. (c) Watanabe, M.; Lizuka, F.; Asada, M. *Japan. J. Appl. Phys. Part 1* **1995**, *34*, 4380.

(7) (a) Ayyappan, S.; Subbanna, G. N.; Rao, C. N. R. *Solid State Ionics* **1996**, *84*, 271. (b) Ayyappan, S.; Rao, C. N. R. *Eur. J. Solid State Inorg. Chem.* **1996**, *33*, 737. (c) Chatterjee, A.; Chakravorty, D. *Appl. Phys. Lett.* **1992**, *60*, 138.

(8) (a) Yeadon, M.; Yang, J. C.; Gibson, J. M. *Appl. Phys. Lett.* **1997**, *71*, 1631. (b) Qi, J.; Ma, J.; Shen, J. *J. Colloid Interface Sci.* **1997**, *186*, 498. (c) Huang, H. H.; Xu, G. Q.; Ji, W. *Langmuir* **1997**, *13*, 172. (d) Suryanarayanan, R.; Frey, C. A.; Buhro, W. E. *J. Mater. Res.* **1996**, *11*, 449. (e) Bigot, J.-Y.; Merle, J.-C.; Daunois, A. *Phys. Rev. Lett.* **1995**, *75*, 4702. (f) Tanori, J.; Pileni, M. P.; *Adv. Mater* **1995**, *7*, 862.

(9) Kimura, K. *J. Colloid Interface Sci.* **1996**, *183*, 607.

(10) Poirier, G. E.; Hance, B. K.; White, J. M. *J. Phys. Chem.* **1993**, *97*, 6500.

(11) (a) Miller, J. M.; Dunn, B.; Pekala, R. W. *J. Electrochem. Soc.* **1997**, *144*, L309. (b) Nashner, M. S.; Frenkel, A. I.; Nuzzo, R. G. *J. Am. Chem. Soc.* **1997**, *119*, 7760.

10.1021/la990015e CCC: $18.00
Published on Web 04/01/1999

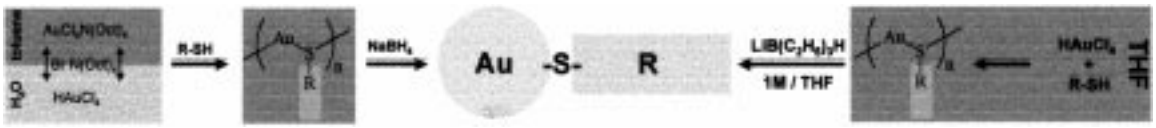

Figure 1. Scheme showing a comparison between the two-phase synthesis (Brust et al.) and the herein presented one-phase synthesis of thiol-functionalized gold nanoparticles.

nanoparticles, opening a new field of self-assembled monolayers. This synthetic route yields air-stable and easy to handle functionalized nanoparticles of moderate polydispersity and is now commonly employed for the preparation of inorganic−organic core−shell composites.

In this method, a quaternary ammonium salt is used to assist in the transfer of the gold $[Au(Cl_4)]^-$ ions, and the $[BH_4]^-$ reducing agent from the water to the organic (toluene) phase (Figure 1). While this method is well suited for the functionalization of the gold colloids with simple *n*-alkanethiols, excessive purification of the decorated particles is required in the case of ω-substituted thiols, forming polar surfaces. In this case, a second layer of the ammonium surfactant covers the nanoparticles and the purification process is long.

A solution to this problem was a one-phase synthesis carried out in methanol as the solvent and sodium borohydride as the reducing agent, as reported by the same group. They have successfully prepared gold nanoparticles covered with 4-mercaptophenol and performed a successive reaction on the shell surface, thereby broadening the application of functionalized gold nanoparticles from a stable but chemically inert compound toward a truly functional reagent. However, methanol is not the ideal solvent for the broad variety of ϖ-functionalized alkane- or arenethiols that is available, simply because of solubility issues. For example, some 4′-substituted-4-mercaptobiphenyls are not soluble enough in both toluene and methanol. This fundamental restriction prevents a full exploitation of the developed synthesis leading to optimal self-assembled systems. An alternative to introducing chemical functionalities into the alkyl shell is a postsynthesis exchange reaction, successfully employed by several research groups.[15] While the exchange strategy can be employed to obtain multifunctional ligand shells, the synthesis of homogeneous (functionalized) thiol shells other than inert *n*-alkyl derivatives is till now restricted to a few examples.[16]

Therefore, we explored possible reducing agents that are soluble in organic solvents, while giving reaction products that are also soluble in organic solvents, and thus can be washed away (Figure 1). In this paper we report a facile one-phase preparation of gold, iridium and palladium nanoparticles, in surfactant-free conditions, using tetrahydrofuran (THF) as a solvent. We describe a synthesis, using *n*-octadecanethiol ($C_{18}H_{37}-SH$, ODT), in order to allow a direct comparison of the product obtained by means of the new preparation with already reported properties of products of the two-phase synthesis. We further report that this route allows for the formation of other aliphatic and aromatic thiol-functionalized gold nanoparticles that cannot be prepared by the usual two-phase synthesis or the one-phase synthesis in methanol.

Experimental Section

Chemicals. All chemicals were purchased from Aldrich and used as received. Solvents were obtained from EM Science or Aldrich. THF used for the synthesis was freshly distilled to remove the stabilizer, which was found to obstruct analysis of the FTIR spectra.

Preparation of Octadecanethiol-Functionalized Gold Nanoparticles. A 235 mg (0.82 mmol) sample of octadecanethiol ($C_{18}H_{37}SH$, ODT) was added under vigorous stirring to a solution of 0.9 mmol of hydrogen tetrachloroaureate(III) trihydrate ($H[Au(Cl_4)]\cdot 3H_2O$) in 10 mL of freshly distilled, anhydrous THF. The reaction mixture was stirred for approximately 20 min at room temperature, before a 1.0 M solution of lithium triethylborohydride in THF was added dropwise. The mixture turned dark red-brown immediately. The addition of the reducing agent was continued at increasingly slower rate, until no more gas evolution could be observed. All other thiol-functionalized gold nanoparticles were prepared using the same procedure.

Preparation of Octadecanethiol-Functionalized Palladium Nanoparticles. A 0.426 g (1.5 mmol) sample of ODT was added, under vigorous stirring, to a solution of 0.336 g (0.5 mmol) of palladium(II) acetate trimer ($[Pd(C_2H_3O_2)_2]_3$) in 10 mL of freshly distilled THF. The solution immediately turned light brown and was stirred for an additional 30 min. "Superhydride" (8 mL) was added, and the reaction mixture was stirred for 2 h more, at which point it was dark brown.

Preparation of Octadecanethiol-Functionalized Iridium Nanoparticles. A 0.186 g (0.5 mmol) sample of dihydrogen hexachloroiridate(IV) $H_2IrCl_6\cdot H_2O$ was added under vigorous stirring to a solution of 0.142 g (0.5 mmol) of ODT in 10 mL of freshly distilled THF under nitrogen. The color of the mixture turns reddish brown. A 7 mL aliquot of "superhydride" was added dropwise to the solution, which turned light greenish brown and became more homogeneous. Stirring continued for 2 h.

Purification of Thiol-Functionalized Nanoparticles. In a general procedure, the resulted solution mixture is evenly divided and poured into two centrifuge tubes, each filled with 20 mL of dry ethanol. The nanoparticles are precipitated, and the supernatant is discarded. This process is repeated until the supernatant is free of thiol or disulfide, as confirmed by thin-layer chromatography (TLC, with hexane as eluent in the case of ODT. The purified material was dried in a vacuum desiccator overnight.

Transmission Electron Microscopy (TEM). Thin films of functionalized gold, palladium, and iridium nanoparticles solutions (in THF for Au/ODT and in $CHCl_3$ for Pd/ODT and Ir/ODT) were drop cast onto a 300 mesh carbon supported film copper grid. Bright field images were obtained using the Philips CM200FEG at 200 keV beam energy for the high-resolution

(12) (a) Fan, H.; Zhou, Y.; Lopez, P. *Adv. Mater.* **1997**, *9*, 728. (b) Giersig, M.; Ung, T.; Mulvaney, P. *Adv. Mater.* **1997**, *9*, 570. (c) Sato, T.; Ahmed, H.; Johnson, B. F. G. *J. Appl. Phys.* **1997**, *82*, 696. (d) Yonezawa, T.; Sutoh, M.; Kunitake, T. *Chem. Lett.* **1997**, 619. (e) Majumdar, D.; Kodas, T. T.; Glicksman, H. D. *Adv. Mater.* **1996**, *8*, 1020. (f) Foss, C. A.; Hornyak, G. L.; Stockert, J. A. *J. Phys. Chem.* **1994**, *98*, 2963. (g) Badia, A.; Gao, W.; Reven, L. *Langmuir* **1996**, *12*, 1262. (h) Badia, A.; Demers, L.; Reven, L. *J. Am. Chem. Soc.* **1997**, *119*, 11104. (i) Reven, L *J. Mol. Catal.* **1994**, *86*, 447.

(13) (a) Evenson, S. A. Badyal, J. P. S. *Adv. Mater.* **1997**, *9*, 1097. (b) Penner, R. M.; Li, W.; Hsiao, G. S. *J. Phys. Chem.* **1996**, *100*, 20103. (c) Gotschy, W.; Vonmetz, K.; Aussenegg, F. R.; *Opt. Lett.* **1996**, *21*, 1099. (d) Korgel, B. A.; Fullam, S.; Connolly, S.; Fitzmaurice, D. *J. Phys. Chem. B* **1998**, *102*, 8379.

(14) (a) Brust, M.; Walker, M.; Bethell, D.; Schiffrin, D. J.; Whyman, R. *J. Chem. Soc., Chem. Commun.* **1994**, 801. (b) Brust, M.; Fink, J.; Bethell, D.; Schiffrin, D. J.; Kiely, C. J. *J. Chem. Soc., Chem. Commun.* **1995**, 1655. (c) Brust, M.; Bethell, D.; Schiffrin, D. J.; Kiely, C. J. *J. Adv. Mater.* **1995**, *7*, 795. (d) Bethell, D.; Brust, M.; Schiffrin, D. J.; Kiely, C. J. *J. Electroanal. Chem.* **1996**, *409*, 137.

(15) (a) Hostelter, M. J.; Green, S. J.; Stokes, J. J.; Murray, R. W. *J. Am. Chem. Soc.* **1996**, *118*, 4212. (b) Andres, R. P.; Bielefeld, J. D.; Henderson, J. I.; Janes, D. B.; Kolagunta, V. R.; Kubiak, C. P.; Mahoney, W. J.; Osifchin, R. G. *Science* **1996**, *273*, 1690. (c) Ingram, R. S.; Hostetler, M. J.; Murray, R. W. *J. Am. Chem. Soc.* **1997**, *119*, 9175.

(16) (a) Johnson, S. R.; Evans, S. D.; Mahon, S. W.; Ulman, A. *Langmuir* **1997**, *13*, 51. (b) Buining, P. A.; Humbel, B. M.; Philipse, A. P.; Verkleij, A. J. *Langmuir* **1997**, *13*, 3921. (c) Reference 14c.

images (Au/ODT), and the Phillips CM-12 transmission electron microscope (100 kev) to determine the average particle size for the Pd/ODT and Ir/ODT nanoparticles. NIH image (Beta 3 release) was used to determine the interparticle spacing.

Electron Diffraction. Normal incidence selected area electron diffraction (SAED) patterns were obtained using the Phillips CM-12 transmission electron microscope (100 kev).

Infrared Spectra. Infrared spectra were recorded on a Nicolet 760 spectrometer with 2 cm^{-1} resolution in transmission mode accumulating 200 scans. A solid sample on a KBr crystal was prepared by evaporating a dilute solution of the nanoparticles from THF. The ODT bulk spectrum was recorded under the same conditions. The ODT monolayer spectrum of a freshly prepared SAM (1 μM solution of ODT in ethanol, freshly prepared and cleaned Au(111) surface on a standard microscope slide, 16 h) was obtained by means of external reflection FTIR using a SpectraTech FT-80 grazing angle setup and a polarizer. A total of 2000 scans were collected in p-polarization.

Results and Discussion

The preparation of thiol-functionalized gold nanoparticles using dry, freshly distilled THF was straightforward. Hydrogen tetrachloroaureate(III) trihydrate ($H[Au(Cl_4)]\cdot 3H_2O$) is soluble in THF, and hence the preparation of the thiolate−gold polymer could be carried out in small volumes of solvent. The addition of lithium triethylborohydride (2 M in THF) resulted in an exothermic reaction, and therefore we employed a jacketed flask and used a thermostatic bath to maintain constant temperature. Detailed studies were carried out at different temperatures;[17] however, the preparations described here were all carried out at room temperature.

The high-resolution transmission electron microscopy (HRTEM) micrograph of a drop-cast nanoparticle film (Figure 2a) displays a representative selection of the crude and *unfractionated* material, with nanoparticles that appear to be nearly spherical. A representative detailed section of the image in Figure 2a (Figure 2b) further corroborate the crystalline nature of these nanoparticles. At this higher magnifications the crystalline nature of the gold cores are visible by the appearance of lattice fringes. The majority of nanoparticles are apparently defect free single crystals. They consist of discrete Au(111) layers with layer spacing of 0.201 nm, which is thus identical to a lattice spacing of bulk metal. Electron diffraction studies (Figure 2c) corroborate this observation and show that the single-crystal gold nanoparticles have the same packing arrangement of bulk gold (fcc). Most of the particles in Figure 2b are slightly elongated, measuring 4 ± 0.3 nm. In comparison to the results of Hostetler et al.[18] using similar reaction conditions (room temperature, $Au(Cl_4)^-$:R−SH ratio, and speed of addition of the reducing agent) we obtain significantly larger gold particles.

The histogram of Figure 2a (Figure 2d) shows size distribution with a peak at 4 nm. The simple drop-cast preparation from a dilute THF solution leads to areas of monolayers of well-ordered 2D assemblies.[19] The size distribution appears to be surprisingly narrow when compared to HRTEM results of similar materials given in the literature. However, a discrete classification of the

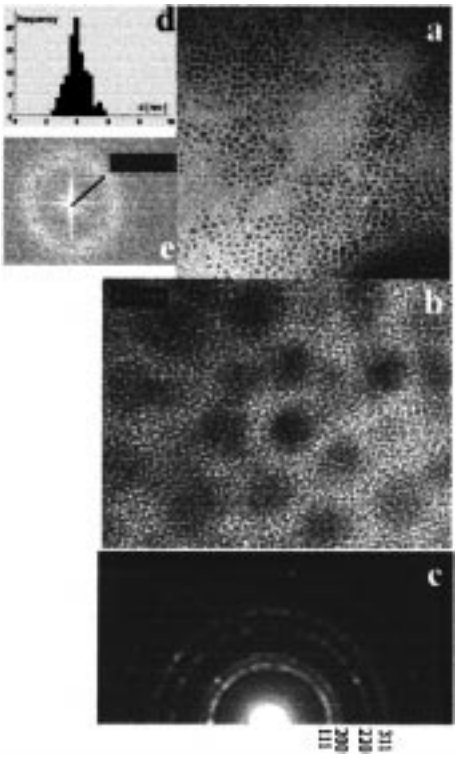

Figure 2. HRTEM micrographs of a nanoparticle monolayer prepared by simple drop-cast from a dilute THF solution (a) and its representative detailed section (b). Electron diffraction (c) shows a fcc structure. The histogram (d) shows size distribution with a peak at 4 nm. The FFT analysis (e) reveals a discrete correlation length of 0.2 nm^{-1}.

particles cannot be made at this point. We found no HRTEM projection of a gold crystallite, which unambiguously displays a geometrically well-defined polyhedral body such as a truncated octahedron, or a similar body classified as energetically stable particle shapes as proposed by Landman and co-workers.[20]

A cylindrical FFT-analysis of the presented picture (Figure 2e) reveals a discrete correlation length of $R = 0.2$ nm^{-1}, which corresponds to an average particle center-to-center distance of 5 nm.[21] It is noteworthy, that the particle edge-to-edge distance was found to be a constant value of 1 nm, which is about half the thickness of a 2D ODT monolayer on a planar Au(111) surface. We have no explanation that can be supported by experimental evidence. Ideas such as interdigitation coupled with considerable tilt may explain this observation. Neutron scattering experiments using gold nanoparticle solutions in different solvents, with a shell of deuterated alkanethiolate moieties are underway. It is hoped that these experiments will provide direct measurements of functionalized gold nanoparticle diameters, and will help resolve the interparticle distance issue.

The UV spectrum of the thiol-functionalized gold nanoparticles is presented in Figure 3. The plasmon band is observed at ~520 nm, in agreement with the average size of the particels.[14] Notice, however, that UV spectroscopy provides limited information on particle size, size distribution, and structure. To investigate the *n*-octade-

(17) Lin, H.; Jordan, R.; Ulman, A. Manuscript in prepration.

(18) Hostetler, M. J.; Wingate, J. E.; Zhong, C.-J.; Harris, J. E.; Vachet, R. W.; Clark, M. R.; Londono, J. D.; Green, S. J.; Stokes, J. J.; Wingall, G. D.; Glish, G. L.; Porter, M. D.; Evans, N. D.; Murray, R. W. *Langmuir* **1998**, *14*, 17.

(19) This simple method was found to produce well-ordered opals from similar (alkanethiol functionalized gold nanoparticles) materials of various particle size dispersities; see: (a) Ohara, P. C.; Leff, D.; Heath, J. R.; Gelbart, W. M. *Phys. Rev. Lett.* **1995**, *75*, 3466. (b) Korgel, B. A.; Fitzmaurice, D. *Phys. Rev. Lett.* **1998**, *80*, 3531.

(20) (a) Reference 9. (b) Luedtke, W. D.; Landman, U. *J. Phys. Chem.* **1996**, *100*, 13323.

(21) Upon closer inspection, a series of individual measurements revealed a particle center-to-center distance of 3.75 to 6.25 nm. However, the variation is obviously caused by the random orientation of the gold particles relative to the plane of projection and does not represent differences in the interparticle order.

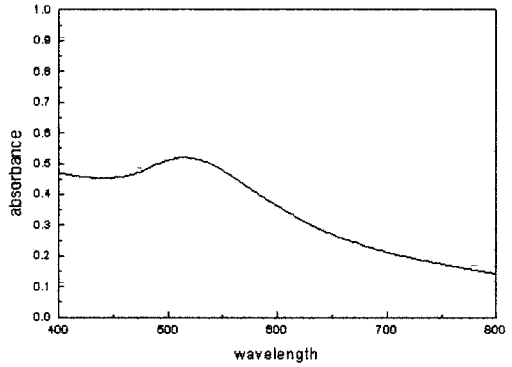

Figure 3. UV spectrum of the thiol-functionalized gold nanoparticles shown in Figure 2. The concentration was 10 mg particles in 10 mL of chloroform.

canethiol-functionalized gold nanoparticles, FTIR spectroscopy was carried out. FTIR is one of the most employed characterization techniques for identification of 2D and 3D SAMs and their characterization with respect to their degree of order and relative orientation. Figure 4 shows the 3100−2700 cm^{-1} CH-stretching region of the infrared spectra of Au:ODT nanoparticles, along with the spectra of a 2D-SAM of ODT on Au(111) and of the bulk ODT for comparison. It is clear that the obtained material is a ODT/Au composite, and combined with the HRTEM results, a gold core-thiol shell model can safely be proposed; this is analogous to particles prepared by the two-phase synthesis.

The positions of the $\nu(CH_x)$ band maxima indicate in all three cases a crystalline solid assembly of ODT molecules. The methyl symmetric and asymmetric stretching modes at 2955 and 2871 cm^{-1} for the bulk ODT and ODT/nanoparticle composite are less pronounced due to the random orientation of the sample molecules, whereas the 2D-SAM spectrum was recorded in p-polarization. The appearance of the methylene stretching modes of Au/ODT particles are not significantly but slightly lower wavenumbers ($\nu_{as}(CH_2) = 2917$ cm^{-1} and $\nu_s(CH_2) = 2849$ cm^{-1}) indicate highly ordered all-trans alkyl chains in the shell surrounding the gold core. This is in agreement with previous studies by Murray et al.[22] and Badia et al.,[23] although a higher degree of gauche defects, and therefore higher band maxima positions in the CH-stretching modes, were reported. The SAM on a gold nanocrystallites has actually more freedom (radius of curvature, "defect" sites at the edges of adjoining Au crystal faces than a 2D-SAM on a planar Au(111) surface[24] and can be expected to exhibit a higher degree of gauche defects that are needed to fill void space. However, besides the higher grafting density (thiol vs *total* surface of the particles is about 30% higher than on a planar Au(111) substrate), interdigitation of individual chains or chain bundles between neighboring particles may provide a mechanism for sufficient crystallization. Since the FTIR experiment has been carried out on a cast nanoparticle film, it does not provide information of the packing and ordering of alkyl chains in a single nanoparticle level. It has to be expected that the interdigitation process becomes more effective when the particles are of similar or even identical size and shape allowing a more efficient as well as uniform packing behavior of particles. As mentioned, the interparticle edge-to edge distance calculates to a constant value of 1 nm which is sterically only possible by a considerable interdigitation/tilt of *n*-alkyl chains. It is noteworthy that such low band positions were only observed when particles were drop-cast from dilute solutions but are unaffected by the type of the solvent used.

The position and shape of the CH_2 bending (scissors) mode between 1475 and 1466 cm^{-1} is known to provide detailed information on the interchain interactions, packing behavior, and therefore the number of gauche defects in an all-trans alkyl chain packing.[25] Badia et al. has reported in a detailed IR spectra analysis of a variety of alkanethiolate:Au nanoparticle $\delta(CH_2)$ positions around 1468 cm^{-1}. The band position is nearly unaffected by the length of the percent chain, indicating that the chains are presumably in a hexagonal subcell packing or a "liquidlike" assembly. In contrast to these studies, we observed a clear band splitting of this mode with band maximum positions at 1473 and 1463 cm^{-1},[26] typical for orthorhombic subcell packing with neighboring chains oriented at about 90° to each other. This organization requires a small amount of defects along the entire chain within the alkyl layer and might only be possible due to the bigger size of the particles itself or/and an efficient match in size and geometry of adjoining particles as well as the absence of contamination.[27]

The unique feature of this new synthetic route is that thiols that are sparingly soluble in toluene or in methanol can be easily used. Figure 5 presents an example of gold nanoparticles functionalized by 4′-bromo-4-mercaptobipheny. A full account of this family of nanoparticles will be published in a forthcoming paper. The synthesis was carried out using the procedure described for Au/ODT nanoparticles, and purification was accomplished using 1:1 THF: ethanol solutions. Figure 5 shows the infrared spectra of 4′-bromo-4-mercaptobiphenyl in bulk (KBr) in a SAM on flat Au(111) surface and in gold nanoparticles. Notice that the 2D-SAM shows a smaller number of bands due to the orientation of the molecules in the monolayer. In all mercaptobiphenyl SAMs, the molecules have a small tilt (≤15°) with respect to the surface normal, and hence all IR bands with transition dipoles parallel to the surface contribute very little to the spectra.

We have mentioned above that using the traditional two-phase route it was difficult to obtain nanoparticles with hydroxy-terminated alkanethiols that show no methyl bands in the FTIR spectrum. Using the superhydride reduction route, on the other hand, purification of such nanoparticles is accomplished simply by washing with ethanol−THF mixtures. Figure 6 presents the infrared spectra of 11-hydroxyundecane-1-thiol in a SAM on flat gold surface, and in gold nanoparticles. Notice that

(22) Hostelter, M. J.; Stokes, J. J.; Murray, R. W. *Langmuir* **1996**, *12*, 3604.

(23) Badia, A.; Cuccia, L.; Demers, L.; Morin, F.; Lennox, R. B. *J. Am. Chem. Soc.* **1997**, *119*, 2682.

(24) For review on SAMs of thiols on gold see: (a) Ulman, A. *An Introduction to Ultrathin Organic Films: From Langmuir−Blodgett to Self-Assembly*, Academic Press: Boston, MA, 1991. (b) Ulman, A. *Chem. Rev.* **1996**, *96*, 1533.

(25) Weers, J. G.; Scheuring, D. R. In *Fourier Transform Infrared Spectroscopy in Colloid and Interface Science*; ACS Symposium Series; American Chemical Society: Washington, DC, 1990.

(26) We have carried out so far synthesis of octadecanethiol-functionalized gold nanoparticles using five different thiol:Au ratios in three different temperatures. The splitting reported here has been consistently observed *only in samples prepared at room temperature using a 1:1 RSH:Au ratio.*

(27) Clearly, more detailed investigations are necessary in order to address the precise packing behavior as well as the nature of the interdigitation process. Studies of the influence of particle size, alkyl chain length, effect of substitutions, and temperature-dependent FT-IR spectroscopy experiments are currently ongoing. At this point only the most striking features and discrepancies of our results which reported once are discussed. A full spectra analysis for all obtained compounds, their dependence on the synthesis, and sample preparation methods will be given in a detailed account.

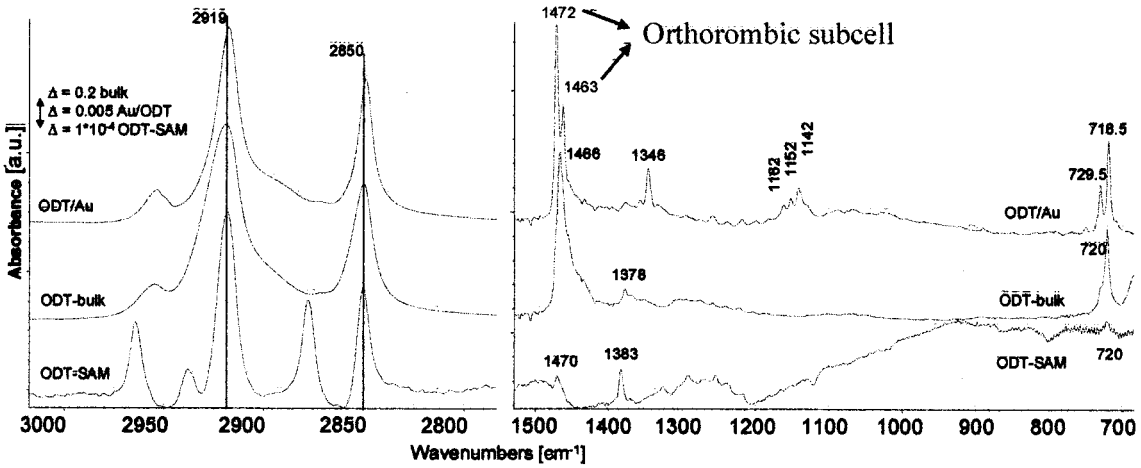

Figure 4. Comparison among external reflection FTIR spectrum of a 2D-SAM of ODT on a planar Au(111) surface, a transmission FTIR spectrum of bulk ODT (KBr pellet), and a transmission FTIR spectrum of a drop-cast film (THF) of Au:ODT nanoparticles on a KBr window.

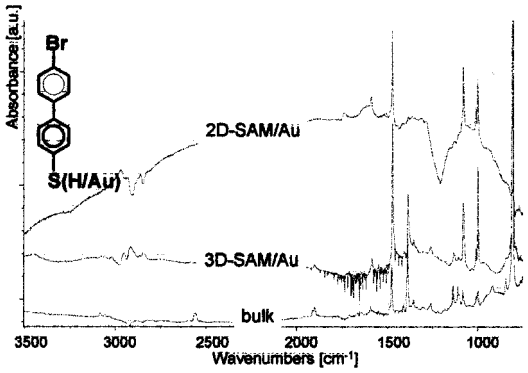

Figure 5. Infrared spectra of 4′-bromo-4-mercaptobiphenyl in bulk (KBr) in a SAM on flat Au(111) surface and in gold nanoparticles.

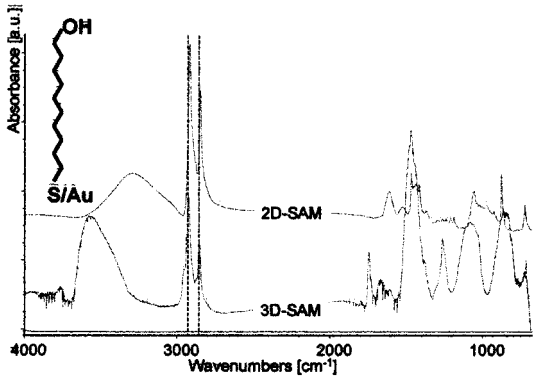

Figure 6. Infrared spectra of 11-hydroxyundecane-1-thiol in a SAM on flat gold surface, and in gold nanoparticles.

only methylene vibrations are observed in the 2800−3000 cm^{-1} region. The other bands are identified with the C−O, CH_2, and OH groups. We have reacted successfully these nanoparticles with trifluoromehane sulfonic anhydride and used the triflated surfaces in surface-initiated ring-opening polymerization.[28] A full account of these studies will be published elsewhere.

Thiol-functionalized palladium[29] and iridium nanoparticles have not been reported yet. We are interested in the availability of different functionalized nanoparticles for both advanced materials and diagnostic applications. Therefore, we are investigating the applicability of the "superhydride" route to the preparation of different metallic nanoparticles.

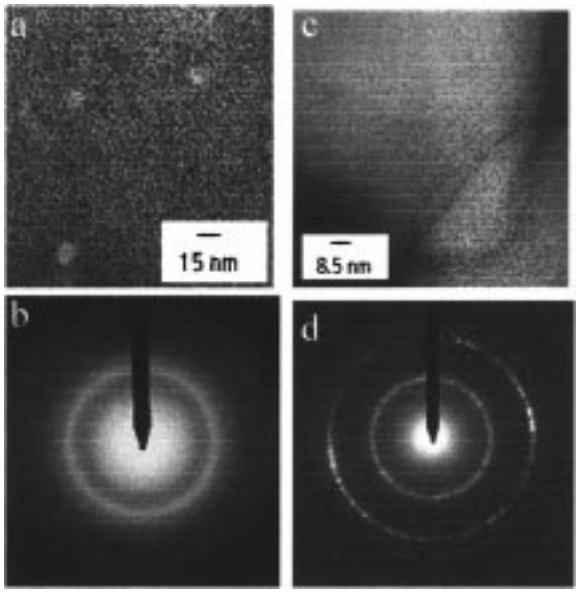

Figure 7. TEM images of Pd/ODT (a) and Ir/ODT (c) nanoparticles. The corresponding electron diffraction results are presented in parts b and d.

The first concern is the solubility of the metallic precursor in THF. Palladium acetate trimer ($[Pd(C_2H_3O_2)_2]_3$) and dihydrogen iridium hexachloride hydrate ($H_2IrCl_6 \cdot H_2O$) are both soluble in THF, and thus the "superhydride" synthetic route may be used. The preparation of both thiol-functionalized nanoparticles was straightforward, and purification of the Pd/ODT and Ir/ODT systems was carried out in ambient atmosphere. The TEM images for Pd/ODT and Ir/ODT nanoparticles are shown in parts a and c of Figure 7. Electron diffraction reveals that both nanoparticles are crystalline (Figure 7b,d), with fcc packing arrangements. The histograms are presented in Figure 8 and show that the average particle size distribution is 2.25 nm for the Pd/ODT, while for the Ir/ODT the distribution is broader with the majority of particles between 2.25 and 4.25 nm. More work needs to be done before control of size and size distribution can be achieved for these new nanoparticle systems.

(28) Jordan, R., Ulman, A. *J. Am. Chem. Soc* **1998**, *120*, 243.
(29) Hidber, P. C.; Helbig, W.; Kim, E.; Whitesides, G. M. *Langmuir* **1996**, *12*, 1375.

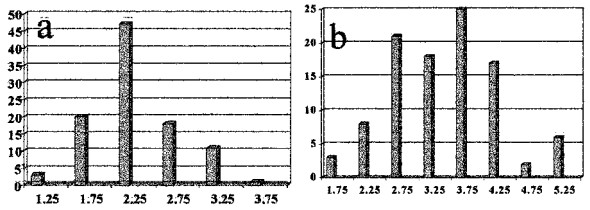

Figure 8. Histograms of Pd/ODT (a) and Ir/ODT (b) nanoparticles.

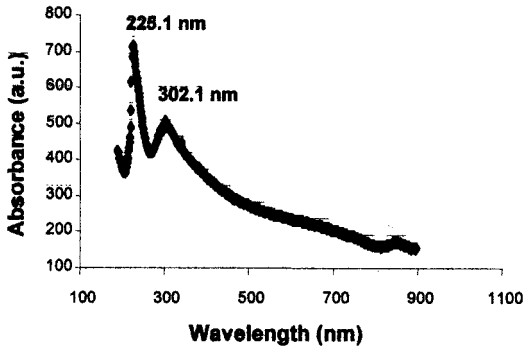

Figure 9. UV spectrum of ODT/Pd nanoparticles in chloroform.

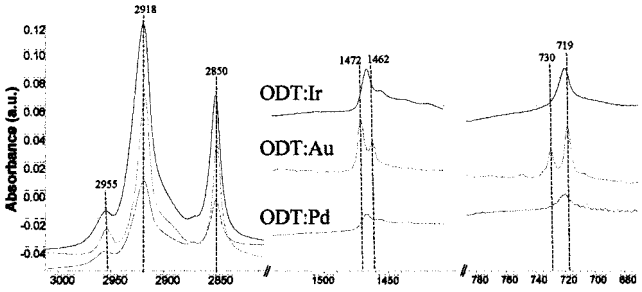

Figure 10. Transmission FTIR spectra of ODT/Pd and ODT/Ir nanoparticles. The spectrum of the ODT/Au nanoparticle is presented for comparison.

The UV spectrum of Pd/ODT nanoparticle in chloroform is presented in Figure 9, showing a plasmon band is at 302 nm. No resolvable band could be observed for the Ir/ODT nanoparticles.

Figure 10 presents the FTIR spectra of Pd/ODT and Ir/ODT nanoparticles. The spectrum of Au/ODT is presented for comparison. Two observations warrant discussion. First, the positions of the $\nu(CH_x)$ band maxima indicate for both Pd/ODT and Ir/ODT a crystalline solid assembly of ODT molecules. The appearances of the $\nu_{as}(CH_2)$ stretching modes of ODT/Ir particles at 2918 cm^{-1} and of Pd/ODT at 2817 cm^{-1} are similar to that of Au/ODT nanoparticles (2817 cm^{-1}). The $\nu_s(CH_2)$ bands appear at 2850 and at 2849 cm^{-1} for the Ir/ODT and Pd/ODT nanoparticles, respectively, again similar to that of Au/ODT (2849 cm^{-1}). These bands suggest highly ordered all-trans alkyl chains in the shell surrounding the iridium and palladium cores.

Second, the position and shape of the CH_2 bending (scissors) mode between 1475 and 1466 cm^{-1} for the Ir/ODT and Pd/ODT nanoparticles is different than for the corresponding Au/ODT nanoparticles. While a clear band splitting of this mode has been observed for the Au/ODT, with band maximum positions at 1473 and 1463 cm^{-1}, typical for orthorhombic subcell packing with neighboring chains oriented at about 90° to each other, there is no clear splitting in both Ir/ODT and ODT Pd spectra. Notice that all samples were prepared by the same procedure, and hence this observation is not an artifact, but represents real differences in the packing of octadecyl chains in the three cases. Since all nanoparticles show fcc packing, these observations may result from differences in the thiolate metal interactions. There is no structural information on 2D-SAMs in both cases, and thus it is not possible at this point to discuss issues such as S···S distance or epitaxy. The Pd/ODT and Ir/ODT nanoparticles are both smaller than that of the Au/ODT, which may provide a partial explanation. Furthermore, that for the Ir/ODT, where size distribution is broader, there is a distinct shoulder may suggest that the observed splitting may be the result of the interdigitation during interparticle contact, as mentioned above. However, these explanations should be supported by more experimental evidence.

Conclusion

A new, facile, general one-phase synthesis for thiol-functionalized gold palladium and iridium nanoparticles using tetrahydrofuran (THF) as the solvent, and lithium triethylborohydride (Superhydride) as the reducing agent, is presented. For octadecanethiol-functionalized gold (Au/ODT) nanoparticles, HRTEM of drop-cast particle films revealed the formation of spherical particles of $d = 4 \pm 0.3$ nm average size. Electron diffraction shows fcc packing arrangement, similar to that of bulk gold. The crystalline gold cores are surrounded with closely packed *n*-alkyl chains mainly in an all-trans conformation, adopting orthorhombic packing as confirmed by FTIR spectroscopy. Particles are arranged in a discrete solidlike assembly with a correlation length of ~5 nm, as the interparticle distance (center-to-center) and a constant edge-to-edge distance of 1 nm as shown by FFT-analysis. Using the same synthetic procedure gold nanoparticles functionalized with 11-hydroxyundecane-1-thiol and with 4′-bromo-4-mercaptobiphenyl were prepared.

TEM images of drop-cast Pd/ODT and Ir/ODT nanoparticles show an average size of 2.25 nm for the former, while for the latter the distribution is broader with the majority of particles between 2.25 and 4.25 nm. Both nanoparticles are crystalline with fcc packing. FTIR spectroscopy reveals that octadecyl chains are close-packed in all-trans conformation, and that there is presumably one chain in unit cell.

Acknowledgment. This work was funded by the NSF through the GRT program (DGE 955452) and the MRSEC for Polymers at Engineered Interfaces. We are grateful to Applied Materials, Inc., of Santa Clara, CA, for allowing us to use their electron microscope.

LA990015E